Nanomagnetism: extension of the Stoner–Wohlfarth model within Néel's ideas and useful plots

2007 J. Phys.: Condens. Matter 19 506201

(http://iopscience.iop.org/0953-8984/19/50/506201)

IOP PUBLISHING JOURNAL OF PHYSICS: CONDENSED MATTER

J. Phys.: Condens. Matter **19** (2007) 506201 (18pp) doi:10.1088/0953-8984/19/50/506201

Nanomagnetism: extension of the Stoner–Wohlfarth model within Néel's ideas and useful plots

M A Chuev[1] **and J Hesse**[2]

[1] Institute of Physics and Technology, Russian Academy of Sciences, 117218 Moscow, Russia
[2] Institut für Physik der Kondensierten Materie, Technische Universität Braunschweig, Mendelssohnstrasse 3, 38106 Braunschweig, Germany

E-mail: chuev@ftian.ru

Received 11 July 2007, in final form 26 September 2007
Published 19 November 2007
Online at stacks.iop.org/JPhysCM/19/506201

Abstract

This paper deals with the extension of the well known Stoner–Wohlfarth (SW) model widely used to compare magnetic properties of real single-domain particle systems with its ideal predictions. The model is often discussed in connection with nanomagnetism. The extension of this successful SW model is gained by combining it with Néel's ideas concerning the dynamical behavior and relaxation of the magnetization in such systems. We present the derivation of a universal relaxation equation which holds for the populations of the SW energy levels defined by the SW model. By solving this differential equation with properly chosen initial conditions, a number of magnetization phenomena observed experimentally versus temperature, time, and external magnetic fields can be understood and described quantitatively. So, hysteresis loops, including those in high-frequency external magnetic fields, can be calculated within this model as a function of temperature, and demagnetization curves for arbitrary heating rates in different external magnetic fields can be simulated. In contrast to the difficulties encountered when treating the experimental data within more general stochastic models based on the Landau–Lifshitz–Gilbert equation, one can easily fit to a first approximation a wide set of data taken from the same sample within the extended SW model. The well known Henkel and Thamm–Hesse plots are reviewed and it is shown that by using these for plotting experimental data deviations from the ideal SW behavior and influences caused by relaxation can be detected. The plot recently proposed by Michele–Hesse–Bremers is shown not to be sensitive to relaxation influences and therefore reveals only the particle–particle interaction.

1. Introduction

For a long time two fundamental ideas have strongly and successfully influenced the understanding and description of the magnetic properties of single-domain fine particles. They

were suggested in the middle of the last century by Stoner–Wohlfarth (SW) [1] and Néel [2]. Whereas SW in their paper neglect any temperature influences and therefore relaxation phenomena, in Néel's fundamental paper these effects are in the foreground. SW introduced their model to understand the coercivity of ferromagnetic alloys made from magnetically soft basic metals but exhibiting 'particles' as precipitations responsible for their magnetic 'hardness'. Néel introduced his ideas in order to understand the magnetic properties of ensembles of small magnetic particles as can be found in geology.

The rapid growth of nanophysics has also strongly influenced the discussion about magnetic properties of small particles and particle ensembles. Now it is possible to speak about 'nanomagnetism' as an essential part of nanophysics in general. It is fortunate that small enough nanoparticles consisting of ferro- or ferri-magnetic materials very often are single-domain particles. Therefore, the basic ideas of Néel and Stoner–Wohlfarth become applicable in a rather 'natural way'. An overview about the typical scales responsible for the formation of single-domain particles can be found in the comprehensive contribution of Hernando [3] and a short introduction into problems of nanomagnetism can be found in [4] together with the literature cited there.

Combining both the ideas of Stoner–Wohlfarth and Néel, marked progress could be achieved. First it was demonstrated that the surprising shapes of Mössbauer spectra collected in radio frequency (rf) magnetic fields on magnetic alloys containing nanoparticles [5] are due to the unusual shape of the magnetic hysteresis loop when considering very fast changes of the external magnetic field [6]. Then, in the next step, a generalization of the Stoner–Wohlfarth model, with a more accurate account taken of relaxation processes, has been performed [7] in accordance with the Néel equation for the relaxation rate between local energy minima divided by an energy barrier U_0 [2]:

$$p = p_0 \exp(-U_0/k_B T), \tag{1}$$

where p_0 is the fluctuation rate, which is slightly dependent on temperature T as compared to the exponent and determined by the basic properties of the particle in question, for instance, it can be defined by the statistical average of rapidly fluctuating random forces and expressed in terms of a 'random field' [8, 9]. The generalization also results in non-trivial shapes of magnetization curves in different frequency ranges [7].

The diversity of techniques to study the non-equilibrium magnetism of nanoparticles and corresponding forms of the temperature and field dependencies obviously supplies one with a large amount of information on physical characteristics inherent to the system studied [4, 5, 10–16]. The only way to extract the information from the experimental data is to define a model of the magnetic dynamics in order to describe the whole set of experimental data for the sample studied. In the general case, such a model can be specified by a system of kinetic equations for magnetization relaxation based on the Landau–Lifshitz–Gilbert equation and a number of simulations of this kind have been reported [9, 17, 18]. However, a real numerical analysis of the experimental data has not yet been performed within this approach due initially to computational problems. Instead, researchers use either the Stoner–Wohlfarth model or Néel model to interpret the experimental data, which often reduces to a finite number of empirical parameters such as the blocking temperature [10–12, 14, 15], the coercivity [14], or magnetic anisotropy constants [13]. In such a situation, the extension of the SW model within the Néel relaxation (1) seems to be a good phenomenological approach applicable for fitting the experimental data and estimating the physical characteristics of samples containing nanoparticles.

The SW model (and also the later introduced extended SW model) predicts the magnetic behavior of an ideal particle system and therefore in the literature it is commonly accepted that

it plays the role of a reference. Its consequences are often compared with magnetization data obtained in experiments on real nanoparticle systems by useful plots directly constructed from the experimental data. These plots will be discussed in this contribution, too.

In this paper we start first with repeating briefly the basic assumptions of the SW model which neglect any thermal activation. In the second part the extended SW model is introduced which includes the Néel possibility for thermal activation and fluctuations of the single-particle magnetic moments within the energy levels defined by the SW model. Then the derivation of a universal relaxation equation which holds for the differences of populations of the SW energy levels follows. The solution of this relaxation equation is presented for the examples of magnetization measurements performed in alternating magnetic field at different temperatures and in an external magnetic field with constant heating rates. In both sections, helpful plots are presented to be used in comparisons of experimental data with those predicted by the ideal SW model and the extended SW model introduced here. We repeat the basic ideas of the Henkel plot [19] and the plot proposed by Thamm and Hesse [20] as well as suggest an explanation of the plot proposed by Michele, Hesse, and Bremers [4, 16] in the framework of the extended SW model. For the calculations, the interaction effects are introduced in the framework using the popular molecular field ansatz.

2. The Stoner–Wohlfarth model

The ideal SW particles are homogeneously magnetized single-domain particles of rotational elliptical shape with uniform magnetization M_0 occupying volume V and, therefore, have a uniaxial (shape) magnetic anisotropy energy density K. In an external magnetic field, the particle's magnetization, being the vector sum of its atomic constituents, rotates homogeneously and behaves like a rigid macroscopic magnetic moment M_0V. The energy density E of such a particle (2) is defined by the anisotropy term and the Zeeman contribution [1]:

$$E = -K\cos^2(\theta - \phi) - HM_0\cos\phi, \tag{2}$$

where θ and ϕ are the angles composed by the external field with the easiest magnetization axis and the magnetization unit vector $\boldsymbol{m} = \boldsymbol{M}/M_0$, respectively (figure 1). For a given particle's properties (M_0 and K) and fixed orientation of the easy axis with respect to the magnetic field, the energy minima determining the position of $\boldsymbol{m}$ can be calculated using (2) for each magnetic field strength. The projection of $\boldsymbol{m}$ on the field direction represents the relative magnetization value. Plotting these dependences versus H delivers reversible magnetization curves for small H values or hysteresis loops when H exceeds a critical value. In the SW model the direction of the particle's magnetic moment lies in the plain defined by the vector of the external magnetic field $\boldsymbol{H}$ and the easy axis.

It is convenient to introduce a reduced dimensionless magnetic field [1]

$$h = \frac{H}{H_C}, \qquad H_C = \frac{2K}{M_0}. \tag{3}$$

Figure 1 (right) shows a series of the particle's energy dependences on the angle ϕ whereas the normalized dimensionless magnetic field strength h acts as a parameter. As seen from the figure, there are two identical local energy minima corresponding to the easy axis direction in the absence of external field. When an external field is applied, the minima shifts over the angle ϕ, i.e. the magnetization tilts away from the easy axis. In weak magnetic fields there remain two energy minima on the curves, while in a reduced magnetic field h is stronger than the critical field depending on the particle's orientation (figure 1, right) and only one local energy minimum survives. (There exists a settle point for $h = 0.5$ and $\phi = -90°$.) The essential

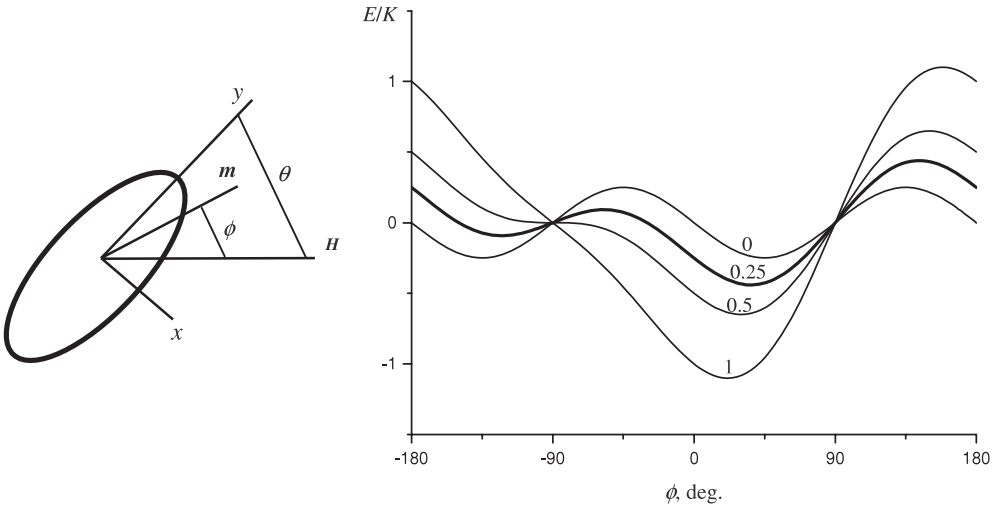

Figure 1. Left: geometric details and angles used to describe the energy density of the magnetization $\boldsymbol{m}$ for a Stoner–Wohlfarth particle with the easy axis fixed in space parallel to the y direction in an external magnetic field $\boldsymbol{H}$. Right: the energy density of an SW particle for a fixed angle $\theta = 45°$ versus the angle ϕ (rotating the particle's magnetization vector). The parameter is the normalized external field h.

assumption of the SW model is that when the external field varies, for definiteness say from positive values of h, the particle's magnetic moment follows the position of and instantaneously changes its direction in accordance with the local minimum and only in a field $h > h_c(\theta)$ passes immediately into the absolute minimum. This actually assumes that there exists an extremely high energy barrier between two local states:

$$U_0 = KV \gg k_B T, \tag{4}$$

where V is the particle's volume, so that according to the Néel equation (1) jumps between these local states at $h < h_c(\theta)$ are supposed to be very slow so that they can be neglected for the measurement time.

When an external periodic magnetic field with normalized amplitude above $h = 0.5$ is applied, the time dependence of the particle's magnetization takes the form of a hysteresis loop. If the amplitude of the periodic field is lower than the minimum critical field $h_c(45°) = 0.5$, then according to the SW model the particle is into one of two local energy minima and never leaves it for the other. The total magnetization curve for an ensemble of the SW particles is naturally the result of averaging over the particles with different orientations as well as over different trajectories within a particular group of particles for which the corresponding value of critical field is larger than the alternative field amplitude.

$$m(H) = \int_0^{\pi} m(\theta, H) \sin\theta \, \mathrm{d}\theta. \tag{5}$$

The simplicity of the SW model allows one to calculate the magnetic properties of a particle ensemble. Because the particles in an SW ensemble are interaction free, their magnetic properties are very often used as a reference for the behavior of systems composed from real particles. Let us now consider some criteria introduced to identify any deviation from the ideal SW particles in the limit without any thermal activation, i.e. when $k_B T \ll KV$ which is also a basic/important assumption of the SW model.

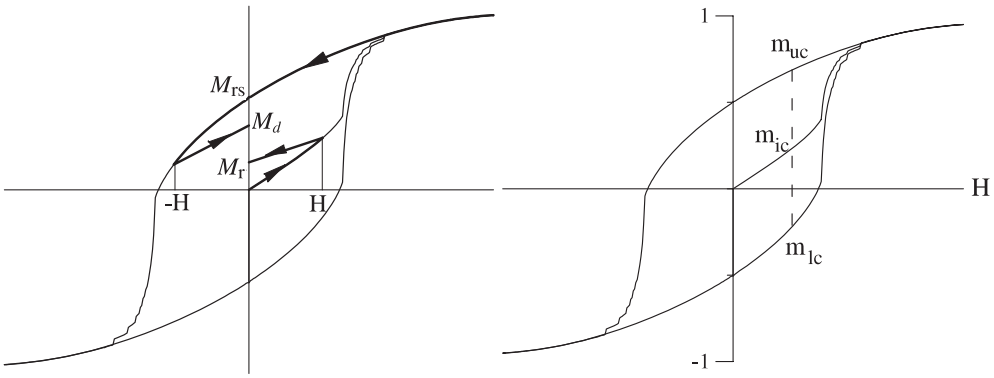

Figure 2. Left: schematic for measuring the remanent magnetizations in order to achieve the Henkel plot. Right: schematic representation of an initial magnetization and the following hysteresis loop in order to achieve the Thamm–Hesse plot.

2.1. Plot proposed by Henkel

Measurements of the remanent magnetization are widely used for comparison of a real particle system's magnetic properties with an ideal SW ensemble. This is often done to characterize interactions between the particles and seldom done to detect deviations from uniaxial anisotropy. Following the suggestion given by Henkel [19], as shown in figure 2 (left), two kinds of remanent magnetization can be distinguished. The demagnetization remanence $M_{\mathrm{d}}(H)$: after saturating the sample by a 'positive' external field $\boldsymbol{H}_{\mathrm{sat}}$, a 'negative' (in the opposite direction) magnetic field $\boldsymbol{H}$ is applied and then switched off, resulting in the remanent magnetization $M_{\mathrm{d}}(H)$. This procedure will be repeated with increasing negative fields until $-H_{\mathrm{sat}}$ is reached leading to $M_{\mathrm{d}}(H_{\mathrm{sat}})$. The magnetization remanence $M_{\mathrm{r}}(H)$: starting with a sample exhibiting $M(H = 0) = 0$ a field $\boldsymbol{H}$ is applied and switched off, resulting in the remanence $M_{\mathrm{r}}(H)$. The procedure is repeated until H_{sat} is reached. The resulting dependences $M_{\mathrm{d}}(H)$ and $M_{\mathrm{r}}(H)$ are usually normalized by the maximum remanence $M_{\mathrm{rs}} = M_{\mathrm{r}}(H_{\mathrm{sat}})$, leading to $m_{\mathrm{d}}(H)$ and $m_{\mathrm{r}}(H)$, respectively.

In an ensemble of ideal SW particles a linear relation between these remanences exists (ideal Henkel plot):

$$m_{\mathrm{d}}(H) = 1 - 2m_{\mathrm{r}}(H). \tag{6}$$

This relation naturally follows from the obvious consequence of the SW model based on equation (2), resulting in the point asymmetry property of the hysteresis curve which for positive H delivers

$$m_{1,2}(\theta, H) = -m_{2,1}(\theta, -H), \tag{7}$$

where $m_{1,2} = M_{1,2}(\theta, H)/M_0$ are the projections of the normalized magnetic moment of the particle on the direction of the magnetic field, corresponding to the local energy minima. For the relative occupation numbers within two local energy minima we obtain

$$w_1(\theta, H_{\mathrm{sat}}) = 1, \qquad w_2(\theta, H_{\mathrm{sat}}) = 0 \tag{8}$$

for the demagnetization remanence scheme and

$$w_1(\theta, H = 0) = w_2(\theta, H = 0) = 1/2 \tag{9}$$

for the magnetization remanence scheme. According to the principal assumption of the SW model given by equation (4), these populations do not change with H decreasing (or increasing) until the value reaches the corresponding $H_c(\theta)$ value. Otherwise, the populations change in a self-consistent way for the two regimes due to equation (7), so that relation (6) must be retained for ideal SW particles at any H and θ values.

Deviations from the linear relation (6) should be evidence for the difference of the real particle system from the ideal SW particle ensemble which may be due to the presence of interactions or a more complex (not uniaxial) magnetic anisotropy.

2.2. Plot proposed by Thamm–Hesse

Because the magnetization measurement, following the suggestion of Henkel, must start from the demagnetized state of the sample, it must be possibile to measure the initial magnetization curve. Thamm and Hesse [20] proposed using this opportunity to measure the initial magnetization curve represented here as a relative magnetization $m_{ic}(H)$ (figure 2, right). After reaching the saturation magnetization only once, a complete hysteresis loop should be measured. From this the upper curve in the first quadrant $m_{uc}(H)$ and the lower curve in the forth quadrant should be used for evaluation. Then the difference indicating any deviation Δm_{TH} from ideal SW behavior is obtained simply by plotting

$$\Delta m_{TH}(H) = m_{ic}(H) - \tfrac{1}{2}[m_{uc}(H) + m_{lc}(H)]. \tag{10}$$

It is easy to see that $\Delta m_{TH} = 0$ for the ideal SW particles results again from equation (7) and initial populations (8) and (9) for the $m_{uc}(H)$ and $m_{ic}(H)$ measurements, respectively, as well as from an additional condition

$$w_1(\theta, -H_{sat}) = 0, \qquad w_2(\theta, -H_{sat}) = 1 \tag{11}$$

for the $m_{lc}(H)$ dependence. In their original paper [20] Thamm and Hesse used the fact that a single SW particle has no explicit initial magnetization curve. The latter appears only in an ensemble of SW particles. An example of measurements performed on a real particle system in a magnetic storage medium can also be found in [20]. It can be found in experiments that the deviation can be positive and negative. A change in sign of the deviation can also appear with the external magnetic field H monotonously growing.

In the Henkel plot one should measure M_{rs} for following the normalization to get the plot, while there is no need in the normalization for the Thamm–Hesse plot. For convenience we used normalized magnetization here. A critical point in both techniques, in the Henkel plot and the Thamm–Hesse plot, is that the experiment must start with a particle system exhibiting the initial zero-magnetization state. Normally, it is very difficult to obtain this zero magnetization. It is often given in a freshly prepared sample. Ideal for such measurements are samples consisting of frozen ferrofluids [4] which can be molten and frozen in zero external magnetic field which allows one to achieve a completely zero magnetized state. The often used AC demagnetization is problematic as experimentally shown in [21].

2.3. Interaction effects in Henkel and Thamm–Hesse plots

In order to demonstrate interaction effects we use the conventional ansatz of the molecular field approximation. Therefore, an internal field proportional to the momentary magnetization is introduced along with an external periodic magnetic field:

$$H(t) = H_0 \sin(\omega_0 t) + bM(t), \tag{12}$$

where H_0 and ω_0 are the field amplitude and angular frequency, respectively, b is the molecular field constant.

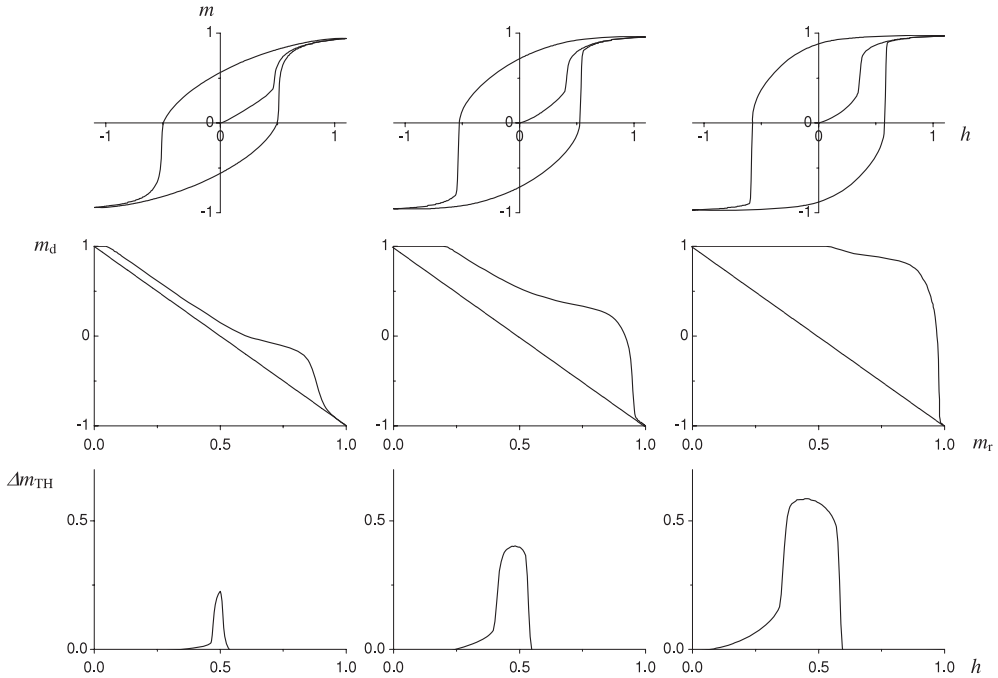

Figure 3. Hysteresis loops (top), Henkel plots (center), and Thamm–Hesse plots (bottom) for an ensemble of 'positive' interacting ($b = 0.1$, 0.3, 0.5 from left to right) SW particles in periodic magnetic field with amplitude $h_0 = 1.1$. Dashed straight lines show the Henkel plots for the non-interacting SW particles.

This internal field may be due to particle–particle interactions with the tendency to form ferromagnetism being a positive interaction ($b > 0$) as well as the demagnetizing field depending on the shape of the macroscopic sample normally being negative ($b < 0$). Negative b values should also be considered when the medium in which the particles are fixed can transmit and influence the particle–particle interactions [4], for example when the medium contains very small particles still behaving like paramagnetic ones whereas the particles under consideration are determining the magnetization of the sample.

Some examples of magnetization curves accompanied with the corresponding Henkel and Thamm–Hesse plots are presented in figures 3 and 4 as calculated within the SW model. As clearly seen from the figures, the positive (ferromagnetic) interaction widens the hysteresis loop while the negative (antiferromagnetic) one makes it narrower. At the same time, the corresponding deviations from the behavior of the ideal non-interacting SW particles grow in the Henkel and Thamm–Hesse plots with the absolute value of interaction parameter b increasing.

Note that rather non-trivial hysteresis loops can be realized for a stronger ferromagnetic interaction between SW particles in complete analogy with the detailed consideration of the case given in [6].

3. The generalized Stoner–Wohlfarth model

In contrast to the Néel idea, the relaxation processes were not directly introduced in the SW model, nevertheless, the relaxation is presented indirectly and plays a rather non-trivial role

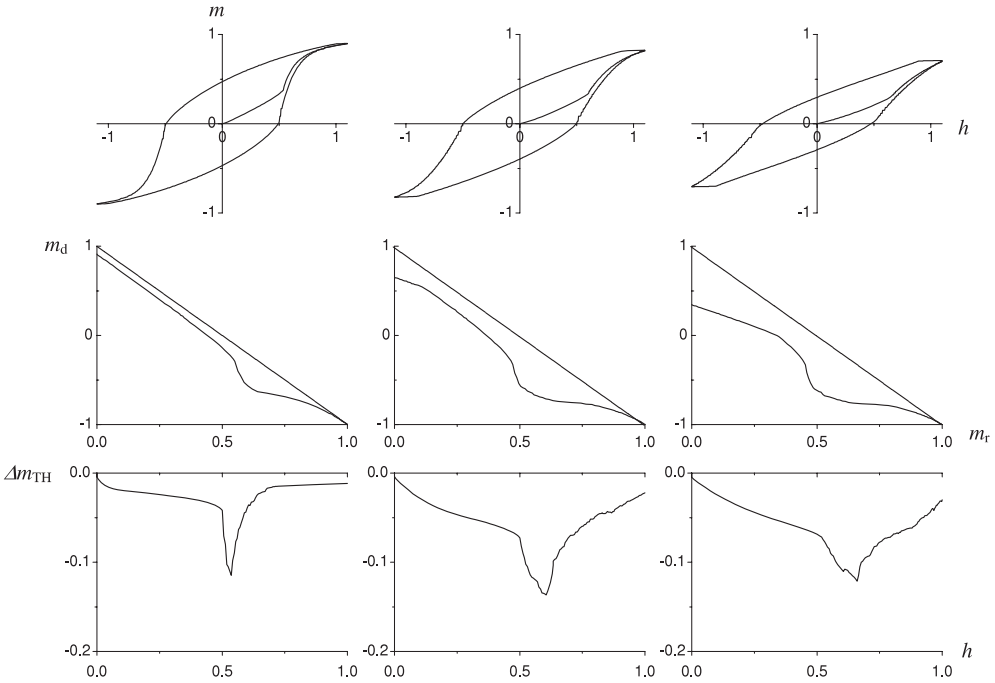

Figure 4. Hysteresis loops (top), Henkel plots (center), and Thamm–Hesse plots (bottom) for an ensemble of 'negative' interacting ($b = -0.1, -0.3, -0.5$ from left to right) SW particles in alternating magnetic field with amplitude $h_0 = 1.1$.

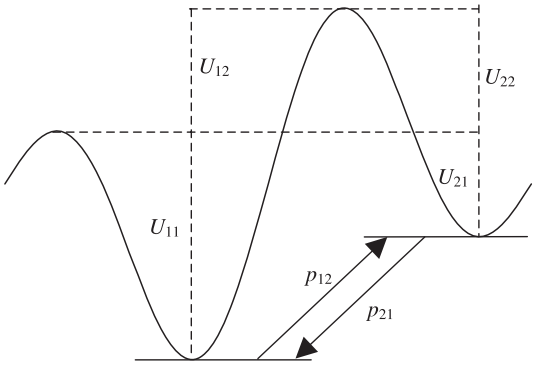

Figure 5. Schematic of the energy barriers and transitions between local energy minima within the generalized SW model.

in this model. Namely, it is assumed that with a magnetic field changing: (i) the particle's magnetic moment being in a definite energy minimum follows the position of the local energy minimum and instantaneously changes its direction in accordance with the strength of the magnetic field applied; (ii) transitions between the states corresponding to different energy minima are forbidden until the strength of the magnetic field becomes stronger than the critical field. In other words, the relaxation process is both extremely fast and extremely slow. The impossibility of jumps between the states with different energy minima is indirectly substantiated by the presence of high energy barriers U_i hampering the jumps (see figure 5).

However, this assumption appears to be valid in a wide range of magnetic fields weaker than h_c, but that must be wrong in the vicinity of the critical field.

A more accurate description of the relaxation process within the SW model has been suggested in [6], where the reorientation of the particle's magnetic moment is regarded to occur not only in a magnetic field stronger than $h_c(\theta)$, but also in weaker fields when the effective energy barriers U_i are not too high as compared to the thermal energy. Such a generalization of the SW model results in a successful description of the remarkable changes in both the magnetic properties and shape of Mössbauer spectra of SW particles [7].

In accordance with the results of [6] and the Néel equation (1), we will assume that depending on the strength of magnetic field in each moment the relaxation process is defined by only two parameters

$$p_{12}(\theta, H, T) = \frac{p_0}{2} \sum_{i=1,2} \exp[-U_{1i}(\theta, H)/k_B T] \tag{13a}$$

and

$$p_{21}(\theta, H, T) = \frac{p_0}{2} \sum_{i=1,2} \exp[-U_{2i}(\theta, H)/k_B T], \tag{13b}$$

where

$$U_{ij}(\theta, H) = E_j^{(\max)}(\theta, H) - E_i^{(\min)}(\theta, H). \tag{14}$$

Here, p_{12} and p_{21} make sense of the probabilities of the transitions between the local equilibrium states (figure 5). For each group of particles with different orientations the values of $E_i^{(\max)}$ and $E_i^{(\min)}$ can be estimated by means of uncomplicated numerical calculations. (Note that in contrast to [6] where only the lower energy barrier has been taken into account, we have introduced into equations (13) an average value of relaxation rate of jumps over both the SW barriers in order to better approximate the three-dimensional character of the energy barrier existing in reality.)

This relaxation model has the advantage that the relaxation process as a whole is characterized by only two parameters: the constant p_0 and the height of the energy barrier $U_0 = KV$ in zero field. At the fixed p_0 and extremely high U_0 just the initial SW model is realized, and the higher U_0, the smaller the time interval within which the energy barriers cannot be regarded as small ones. In the limiting case $U_0 \to \infty$ this interval tends to zero. (In the range of small energy barriers a more accurate description of the relaxation processes could be given, when p_0 is no longer a constant and depends on the strength H of magnetic field [22].)

In magnetic fields $|h| < h_c$, each particle can stay only into two states corresponding to the local energy minima between which the relaxation transitions can occur. Then, the relative equilibrium populations of the states are defined by the detailed balancing principles:

$$w_i^{(0)}(\theta, H, T) = \frac{\exp[-E_i^{(\min)}(\theta, H)/k_B T]}{\exp[-E_1^{(\min)}(\theta, H)/k_B T] + \exp[-E_2^{(\min)}(\theta, H)/k_B T]} \tag{15}$$

and the projection of the equilibrium magnetization of the particle on the direction of the magnetic field is determined by the following expression

$$m^{(0)}(\theta, H, T) = w_1^{(0)}(\theta, H, T) m_1(\theta, H) + w_2^{(0)}(\theta, H, T) m_2(\theta, H), \tag{16}$$

where $m_i = M_i(\theta, H)/M_0$ are the projections of the normalized magnetic moment of the particle on the direction of the magnetic field, corresponding to the local energy minima.

Naturally, under the action of an external time-dependent field (which is assumed here to be periodic in time) the true populations of the local states are in general not equilibrium when

the frequency of the field is high enough as compared to the relaxation rate and depend both on the external parameters (H, T, and the rate of changes in one of them) and parameters (K, V, M_0, p_0, and their distributions) inherent to the system studied. So, at each moment the changes in the non-equilibrium populations of the local states, $w_1(t)$ and $w_2(t)$, for a group of particles with the given angle θ in time can be described by two conventional combined equations

$$\frac{\mathrm{d}w_{1,2}(t)}{\mathrm{d}t} = \pm[p_{21}(t)w_2(t) - p_{12}(t)w_1(t)]. \tag{17}$$

Taking into account the obvious equality

$$w_1(t) + w_2(t) = 1, \tag{18}$$

these equations are reduced to the single equation

$$\frac{\mathrm{d}\tilde{w}(t)}{\mathrm{d}t} = -p(t)[\tilde{w}(t) - \tilde{w}^{(0)}(t)] \tag{19}$$

for the difference of the populations

$$\tilde{w}(t) = w_1(t) - w_2(t), \tag{20}$$

which is a typical relaxation equation. Here we have introduced

$$p(t) = p_{12}(t) + p_{21}(t), \tag{21}$$

and

$$\tilde{w}^{(0)}(t) = w_1^{(0)}(t) - w_2^{(0)}(t). \tag{22}$$

The relaxation equation (19) bears the extended Stoner–Wohlfarth model and should be solved together with the initial conditions. Note that we write down the effective relaxation rates $p_{ij}(t)$ in equations (17) and (19) assuming that at each moment t the system exhibits energy barriers depending on $H(t)$ and/or $T(t)$, which results in the time dependence $p(t)$ that is generally determined by equation (13). That is why the kinetic equation can principally describe memory effects depending on initial conditions in a specified scheme of measurements. As we can see below, this circumstance results in a cardinal difference of relaxation effects on the empirical plots for measurements of magnetization in alternating field and demagnetization in heating where the $H(t)$ and $T(t)$ dependencies are realized, respectively.

According with the initial SW model, in a magnetic field stronger than the critical one, $|h| > h_c$, there are already not two local, but only a single absolute energy minimum and the particle gets to the state corresponding to this minimum in a magnetic field stronger than h_c. In this case $\tilde{w}^{(0)}(t) = 1$ and -1 for $h > h_c$ and $h < -h_c$, respectively. Such very well defined states for the particle system can experimentally be achieved by positive high field cooling or negative high field cooling which is described later.

Nonlinear equation (19) should be supplied with the boundary conditions which are determined by the concrete experimental scheme (see below) applied to study magnetic properties. If $\tilde{w}(t)$ is known, the time evolution of the magnetization of a group of particles with the given angle θ is determined by

$$m(t,\theta) = w_1(t,\theta)\cos\phi_1(\theta) + w_2(t,\theta)\cos\phi_2(\theta), \tag{23a}$$

where

$$w_{1,2}(t,\theta) = \frac{1 \pm \tilde{w}(t,\theta)}{2}, \tag{23b}$$

the angels ϕ_1 and ϕ_2 correspond to the local energy minima. In order to determine the evolution of the total magnetic moment of an ensemble of randomly oriented and non-interacting SW particles, it is necessary to carry out the sum

$$M(t) = M_0 \int m(t,\theta)\sin\theta\,\mathrm{d}\theta. \tag{24}$$

There always exists a distribution of particle sizes $P(V, \sigma_V)$ with a certain width σ_V in a real samples, so that one has also to perform an averaging over the distribution

$$\bar{M}(t) = \int M(t) P(V, \sigma_V)\, \mathrm{d}V. \tag{25}$$

The generalization of the relaxation process in the SW model results in essential changes in the nonlinear magnetic properties and, first of all, in the shape of hysteresis loops [7].

Whereas the relaxation equation (19) for the differences of populations generally holds, the situation for the magnetization is more complex as can be seen in equation (23). Considering the very special case of a system of identical completely textured SW particles with the easy axes parallel to the external magnetic field, the kinetic equation is strongly simplified [6]:

$$\frac{\mathrm{d}m(t)}{\mathrm{d}t} = -p(t) \cdot [m(t) - m_0(t)], \tag{26}$$

where $m(t) \equiv \tilde{w}(t)$ and $m_0(t) \equiv \tilde{w}_0(t)$. This very special case was considered in the introductory part of [4] whereas all calculations must be done and were performed using equation (19).

3.1. Magnetization curves in alternating magnetic filed

The magnetization curve in the initial SW model is determined by only the amplitude of alternating magnetic field (12) and does not depend on either its frequency or the temperature at which the curve is measured. In the extended SW model presented above, the shape of hysteresis loops already becomes dependent on the magnetic field frequency due to relaxation processes being taken into account, i.e. of the ratio ω_0/p_0 as well as of the value of the effective energy barrier $U_0/k_\mathrm{B}T$ [7]. In particular, a simple physical explanation of the widening of the hysteresis loop (increase in the effective switching field) with increasing frequency ω_0 has been given: at lower frequencies ω_0 the SW particles have more time to come into the equilibrium state and the corresponding switching field appears to be weak, while at higher frequencies the particles' magnetic moments have no time to populate the local energy levels in accordance with their equilibrium population so that a stronger field amplitude H_0 is necessary for the particles' magnetization reversal. This fact has been directly associated with a large difference between the switching fields for the widely used soft magnetic Permalloy evaluated from the Mössbauer experiments under radio frequency field excitation (H_c is about several oersted [23]) and from conventional magnetization measurements at low frequencies where H_c only equals about several hundredth of an oersted.

Now we discuss the temperature dependence of the hysteresis shape of magnetization curves for an ensemble of nanoparticles. One can find a number of experimental data of the kind (e.g. the most pronounced set in [18]), however, the treatment of the data used is restricted by the only parameter, the coercive field, which obviously gives very poor information about such complicated systems as an ensemble of nanoparticles. In contrast to the simplest analysis, the extended SW model described above supplies one with a rather powerful tool to extract much more detailed information about the system studied from the experimental magnetization curves. In order to calculate the curves one should solve the kinetic equation (19) with boundary conditions which are given by the periodicity condition when $h_0 < h_\mathrm{c}(\theta)$:

$$\tilde{w}(t + 2\pi/\omega_0) = \tilde{w}(t), \tag{27a}$$

or by the initial condition

$$\tilde{w}(\pi/2\omega_0) = 1 \tag{27b}$$

if $h_0 \geqslant h_\mathrm{c}(\theta)$.

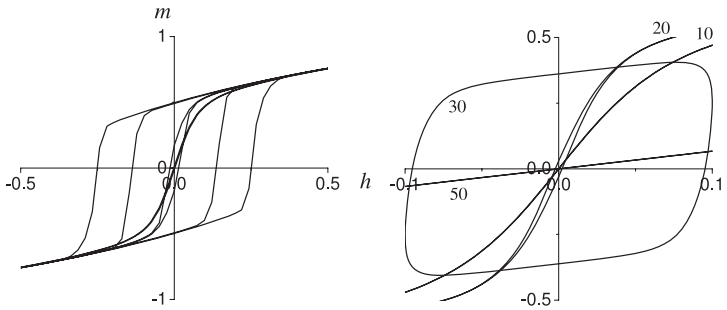

Figure 6. Magnetization curves in an alternating magnetic field with the amplitude $h_0 = 1$ (left) and 0.1 (right) as calculated within the generalized SW model ($p_0/\omega_0 = 10^{10}$) for an ensemble of non-interacting particles with $U_0/k_BT = 10, 20, 30, 50$ (from the inner hysteresis loop to the outer one in the left panel and figures in the right one).

For instance, figure 6 shows the hysteresis loops for an ensemble of SW particles calculated within the extended SW model as a function of the effective energy barrier U_0/k_BT (which at fixed values of U_0 can be regarded as the temperature dependence). As clearly seen from the figure, for $H_0 > H_c$ the hysteresis loops become broader with the effective energy barrier U_0/k_BT increasing (temperature decreasing), which qualitatively correspond to the behavior observed in the experimental temperature-dependent magnetization curves [14] so that the latter can be treated within the extended SW model.

In weak alternating magnetic fields with amplitudes smaller than $H_c/2$ the shape of the hysteresis loops as a function of the periodic field frequency changes in a more complicated manner (figure 6, right). At lower energy barriers (high temperatures) the hysteresis loop broadens with the temperature decreasing by analogy with the case shown in figure 6, left. At extremely high energy barriers (low temperatures) when the relaxation process becomes vanishing, a reversible curve of paramagnetic type is observed instead of the hysteresis loop. And in an intermediate range of energy barriers (temperatures), hysteresis loops of an exotic form are observed (see figure 6, right).

Such a major changes in the shape of hysteresis loops calculated within the extended SW model should naturally be revealed in the Henkel and Thamm–Hesse plots. Examples are shown in figure 7. As seen from the left column of the figure, even in the absence of interaction, deviations of the plots from those characteristic of an ensemble of ideal SW particles are observed, the signs of changes being opposite. It is clear that these changes in the plots are only due to relaxation effects. With increasing interaction parameter the hysteresis loop becomes broader and the shape of plots changes towards that for the initial SW model. However, in contrast to the latter, drastic changes in the plots occur at the external field strength not around the minimal value of $h_0 = h_c(45°) = 0.5$ (see figure 3), but in a somewhat weaker field (figure 7).

A detailed consideration of the problem is out of the frame of this paper and will be studied elsewhere. Note only that, as seen from figure 7, the relaxation and interaction effects are revealed on the Henkel and Thamm–Hesse plots in a qualitatively different manner and could be easily distinguished one from the other.

Finally, we should mention that we have to speak about high frequency when the frequency of the external magnetic field becomes comparable to or larger than the relaxation rate. The momentary relaxation rate in the interaction-free SW model is dependent only on the temperature and is independent of the initial state of the magnetization. This situation changes

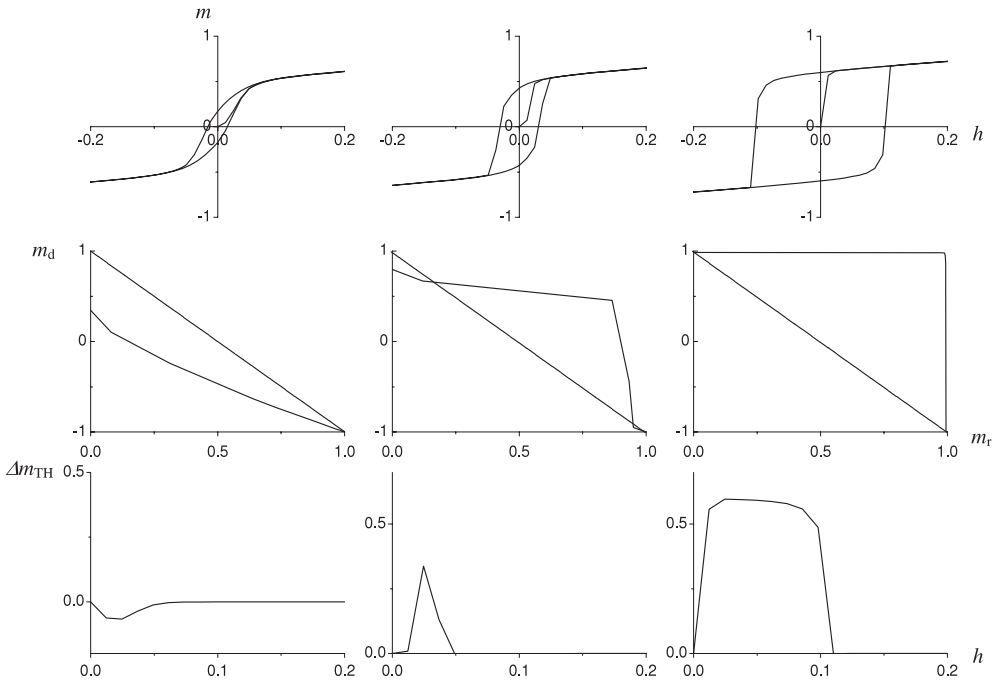

Figure 7. Hysteresis loops (top), Henkel plots (center), and Thamm–Hesse plots (bottom) for an ensemble of nanoparticles as calculated within the generalized SW model ($h_0 = 1$, $U_0/k_BT = 20$, $p_0/\omega_0 = 10^{10}$) for different values of the interaction parameter $b = 0, 0.1, 0.3$ (from left to right).

if the interactions start to become important. Then the relaxation rate becomes dependent on the momentary field and magnetization.

3.2. Demagnetization curves in heating

There exists one more highly informative technique to study non-equilibrium magnetism of nanoparticle systems, i.e. measurements of temperature dependence of their magnetization during heating in external magnetic fields (field warming (FW)) after cooling in different regimes in order to reach a different, but well-defined low-temperature state of the system studied [4, 12, 24, 25]. In these papers (for clearer definition) positive high field cooling (PHFC) and negative high field cooling (NHFC) were introduced. This is done in order to have a strict difference to the very often used field cooling (FC) or positive/negative field cooling (PFC/NFC) in more or less arbitrarily chosen magnetic field strengths. In [12] PHFC means cooling the sample in a field strong enough to populate only magnetic moment states with moments oriented parallel to the external field. In this cooling procedure, down to a temperature below the blocking temperature of the particles, the sample is prepared in a well-defined magnetic state. From this, the warming in external magnetic fields FW starts (the field strength now can be chosen very differently to the cooling process and has to regard also small values). For such a procedure the abbreviation PHFC ‖ FW was introduced. NHFC also requires preparing the sample in a well-defined magnetic state but with the difference that now the magnetization is opposite to the field orientation applied during heating the sample. Also, for such a procedure the abbreviation NHFC ‖ FW is used. Whereas the procedures of PHFC and NHFC always lead to a well-defined ‘starting state’ of the sample, the often

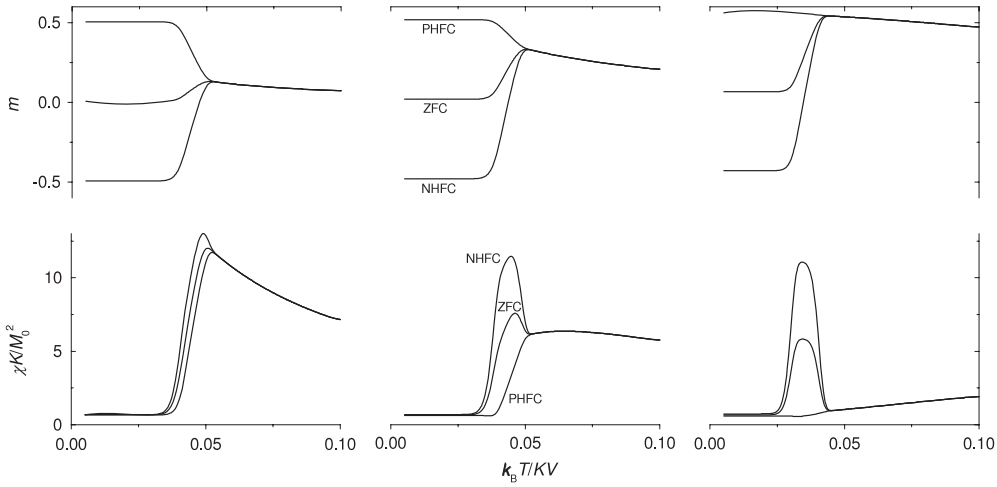

Figure 8. Demagnetization curves PHFC ∥ FW, ZFC ∥ FW, and NHFC ∥ FW (top) and differential susceptibilities (bottom) in heating for different strengths of applied magnetic field $h = 0.01$ (left), 0.03 (center), and 0.1 (right) in different cooling regimes as calculated within the generalized SW model ($p_0/(\Delta T/\Delta t) = 10^9$ K^{-1}).

used FC procedures described in the literature only use intermediate field strength values and therefore start with samples exhibiting different populations of both energy levels in the SW model. Therefore, we do prefer PHFC and/or NHFC together with zero field cooling (ZFC) in the following considerations.

In contrast to the initial SW model, which cannot completely describe this type of magnetic measurement, one can simulate these curves within the extended SW model given above. Indeed, we can use the same kinetic equation (19) in order to describe the temporal changes in non-equilibrium populations of local energy states, assuming that their time dependence is defined not by an alternative field (12), but by the temperature changing in time, e.g.

$$T(t) = T_0 + (\Delta T/\Delta t)t, \tag{28}$$

where T_0 is the temperature at which the heating starts, and $(\Delta T/\Delta t)$ is the rate of changes in temperature. In order to calculate the demagnetization curves in heating, one should solve equation (19) with boundary conditions which in this case are the initial conditions defined by the cooling procedures:

$$\tilde{w}_j(T_0) = 1, 0, -1, \tag{29}$$

for PHFC, ZFC, and NHFC.

Then, using equations (19)–(25), (28), and (29), one can calculate the temperature dependence of demagnetization for an ensemble of nanoparticles within the extended SW model as a function of the internal parameters K, V, σ_V, p_0 provided that the external parameters H, T_0, and $(\Delta T/\Delta t)$ are given. Figure 8 shows an example of the demagnetization curves for different cooling procedures as a function of the applied magnetic field. As clearly seen from the figure, these curves qualitatively reproduce the behavior observed in the experimental temperature-dependent demagnetization curves [4, 12, 24] so that the experimental data can be largely treated within the extended SW model.

The difference between cooling regimes PHFC ∥ FW, ZFC ∥ FW, and NHFC ∥ FW is most pronounced in the corresponding temperature dependences of magnetic susceptibilities

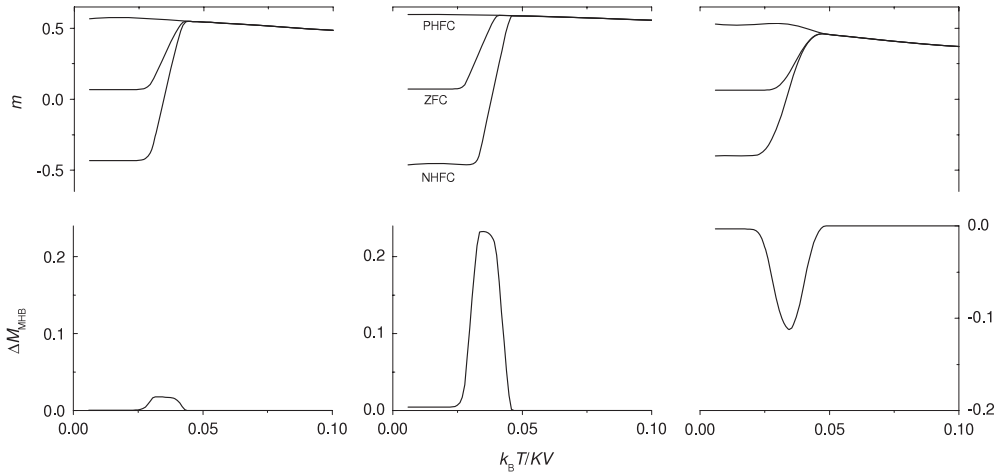

Figure 9. Demagnetization curves in heating within different cooling regimes PHFC ∥ FW, ZFC ∥ FW, and NHFC ∥ FW (top) and corresponding Michele–Hesse–Bremers plots (bottom) for different values of the interaction parameter $b = 0.01$ (left), 0.1 (center) and -0.1 (right) as calculated within the generalized SW model ($h = 0.1$, $p_0/(\Delta T/\Delta t) = 10^9\ \mathrm{K}^{-1}$).

calculated within the extended SW model in accordance with the definition given in [12] which in general reads

$$\chi(T, H) = \lim_{\Delta H \to 0}\left[\frac{M(T, H + \Delta H) - M(T, H)}{\Delta H}\right]. \tag{30}$$

The dimensionless value $\chi(T, H) \cdot K/M_0^2$ is plotted in figure 8, bottom. These curves can be very helpful in understanding and treating the temperature dependences of differential magnetic susceptibilities experimentally evaluated for systems with magnetic nanoparticles [12, 24].

3.3. Universality of the kinetic equation and plot proposed by Michele–Hesse–Bremers

As one can see from the previous two sections, the kinetic equation (19) appears to be universal for descriptions of a number of experimental data collected using different techniques. Moreover, as has been found empirically [4, 16], there exists one more plot in order to test the presence or absence of interaction within the measurements of the temperature dependence of magnetization of nanoparticles in heating after definitive cooling in different regimes. Michele, Hesse, and Bremers [4, 16] have shown that for non-interacting SW particles the following relation holds:

$$m_{\mathrm{ZFC}\|\mathrm{FW}}(T) = \tfrac{1}{2}[m_{\mathrm{PHFC}\|\mathrm{FW}}(T) + m_{\mathrm{NHFC}\|\mathrm{FW}}(T)]. \tag{31}$$

In an real particle system, therefore, it becomes sensible to plot the following deviation:

$$\Delta m_{\mathrm{MHB}}(T) = m_{\mathrm{ZFC}\|\mathrm{FW}}(T) - \tfrac{1}{2}[m_{\mathrm{PHFC}\|\mathrm{FW}}(T) + m_{\mathrm{NHFC}\|\mathrm{FW}}(T)]. \tag{32}$$

For instance, figure 9 shows an example of the demagnetization curves in heating for different cooling regimes calculated within the generalized SW model for different values of the interaction parameter b, accompanied by the corresponding Michele–Hesse–Bremers plots. As clearly seen from the figure, the presence of interaction breaks the condition (31), the corresponding deviation (32) being larger with increasing interaction parameter b. Moreover, the sign of the deviation is opposite for positive and negative b values.

Such a behavior is qualitatively clear. In the presence of 'positive' interaction, at the starting point of measurements (at low temperatures) an ensemble of interacting SW particles in the PHFC ∥ FW regime is under a stronger effective magnetic field as compared to that in the NHFC ∥ FW regime, which is in accordance with equation (12). This situation remains with temperature decreasing so that the equilibrium state of the system in the PHFC ∥ FW regime is reached at lower temperatures than that in the NHFC ∥ FW regime (magnetization in the ZFC ∥ FW regime appears to be in between). For a 'negative' interaction the situation is just the opposite so that the magnetization of an ensemble of interacting SW particles in the PHFC ∥ FW regime is 'delayed' in the temperature at which the equilibrium state is reached (see figure 9). These effects are clearly seen in the corresponding Michele–Hesse–Bremers plots.

In contrast to the Henkel and Thamm–Hesse plots constructed from hysteresis loops, the relaxation does not influence the Michele–Hesse–Bremers plot for a system of non-interacting SW particles. This difference is obviously related to the difference in initial conditions with which the plots are obtained. In magnetization measurements in alternating magnetic field the partial curves based on which the Henkel and Thamm–Hesse plots are constructed are measured starting from different initial states and at different initial strengths of external magnetic field. This results in different initial relaxation rates (13) at the starting point of each measurement, which breaks the symmetry of kinetic equation (19). Otherwise, the PHFC ∥ FW, ZFC ∥ FW, and NHFC ∥ FW curves, on which the Michele–Hesse–Bremers plot is constructed, are measured principally at the same values of the field strength H and temperature $T(t)$ so that the symmetry of equation (19) with respect to the given initial conditions remains over the whole temperature range of measurements.

It is easy to see that the Michele–Hesse–Bremers equality (31) directly follows from the universal kinetic equation (19). Indeed, due to the fact that the coefficients $p(t)$ and $\tilde{w}^{(0)}(t)$ depend only on the momentary values of magnetic field and temperature, which are the same for different cooling regimes, this equation can be rewritten for the average value of non-equilibrium difference in populations of local energy states for the PHFC and NHFC regimes

$$\bar{w}_{\mathrm{FC}}(t) = \tfrac{1}{2}[\tilde{w}_{\mathrm{PHFC}}(t) + \tilde{w}_{\mathrm{NHFC}}(t)] \tag{33}$$

in a similar manner:

$$\frac{\mathrm{d}\bar{w}_{\mathrm{FC}}(t)}{\mathrm{d}t} = -p(t)[\bar{w}_{\mathrm{FC}}(t) - \tilde{w}^{(0)}(t)] \tag{34}$$

with the obvious initial condition for a group of SW particles with the given angle θ

$$\bar{w}_{\mathrm{FC}_j}(T_0) = 0. \tag{35}$$

It is clear that equation (34) with the initial condition (35) is nothing more than the kinetic equation for the ZFC regime, i.e. $\bar{w}_{\mathrm{FC}}(t) = \tilde{w}_{\mathrm{ZFC}}(t)$. Then, performing all the summations by means of equations (23)–(25), one comes to the Michele–Hesse–Bremers relation (31) for an ensemble of non-interacting SW particles. As mentioned above, the presence of even a small interaction of any sign will break the symmetry of kinetic equation (19) defined by equations (33)–(35) and result in non-zero deviation (32).

4. Conclusions

This paper has started with the basic assumptions of the Stoner–Wohlfarth model which in its original form neglects any thermal activation in the movement of the magnetic moments. Just the basic SW ideas lead one to useful plots which evaluate the difference between the magnetic

behavior of a SW system acting as a reference in comparison to the real systems. Therefore the Henkel plot and the plot proposed by Thamm–Hesse are discussed and often used in the evaluation of experiments. In the second part the extended SW model is introduced which includes the Néel possibility for thermal activation and fluctuations of the single-particle's magnetic moment. These considerations lead us to a generally valid relaxation differential equation which holds for the population difference of both SW energy levels. In this way the general possibility is offered to describe any magnetic property of the particle system in question in the limit of the basic Stoner–Wohlfarth assumptions, for instance, any type of hysteresis loop collected in slowly changing external magnetic fields (slow in comparison to the relaxation rate) but also the hysteresis loops for rapidly changing external magnetic fields (fast in comparison to the relaxation rate).

On the other hand, any kind of demagnetization of the nanoparticle sample when heating in an external magnetic field can be obtained and treated within the same model. Here we do prefer to start with well-defined low-temperature magnetic states of the particle system in question which can be achieved experimentally by positive high field cooling, negative high field cooling, and zero field cooling, respectively. In this consideration the idea of a new plot, proposed by Michele *et al* [4], is explained within the extended SW model in terms of a general universal relation: in an interaction-free SW particle system the magnetization curve obtained after zero field cooling is the arithmetic middle taken from the magnetization measured after positive high field cooling and negative high field cooling measured in the same external magnetic field with the same heating rate. It should be noted that the extended SW model helps to clarify the principal difference between the classic Henkel (or Thamm–Hesse) plot and the recent Michele–Hesse–Bremers plot because the former is affected by both the magnetization relaxation and inter-particle interaction while the latter is just a consequence of relaxation effects and characterizes the presence or absence of only interactions between particles.

Additional information can be obtained from the Mössbauer spectra collected on magnetic nanoparticles. It was shown in [5, 7] that the spectra measured under rf field excitation can also be treated and understood within the extended SW model with an effective inclusion of the magnetization's precession effects [9]. All the techniques mentioned above can be applied to the same sample, and treatment of the whole set of experimental data collected in the different techniques within the same model of magnetic dynamics must give a lot of information about the system studied, even about a complex system of magnetic nanoparticles. The extended SW model is the tool we propose to solve this problem. It is also clear that a real system containing nanoparticles is always inhomogeneous so that one should inevitably take into account distributions of physical parameters inherent to the system (e.g. particle size distribution [24, 25]) in a treatment of the experimental data within any model of magnetic dynamics. Such a model should also include somehow the temperature dependence of the uniform saturation magnetization $M_0(T)$ characterizing each single particle.

One should keep in mind that, in agreement with the basic assumptions of the SW model, the continuous diffusion and precession of the particle's magnetic moment are also not taken into account in the extended SW model. This will limit the application of the latter in analyzing the experimental data and more general models of magnetic dynamics [8, 9, 17, 18] can essentially correct the results of analysis within the extended SW model mentioned above. However, the main advantage of the model is its simplicity in numerical calculations so that one can easily use it to fit the experimental data and qualitatively estimate the most important physical parameters inherent to the sample studied as well as to obtain a first approximation for further analysis in the framework of more advanced (and much more complicated) models of magnetic dynamics.

Acknowledgments

The authors are grateful to Professor Dr Alexander Afanas'ev (Corresponding Member of Russian Academy of Sciences) for many years of very intensive and fruitful collaboration. He contributed a lot of original and successful ideas which allowed us to understand the magnetic properties of nanoparticle systems including the interpretation of very complex Mössbauer spectra collected in high-frequency magnetic fields.

This work was partially (MCh) supported by the Russian Foundation for Basic Research (project No. 05-02-16297).

References

[1] Stoner E C and Wohlfarth E P 1948 *Phil. Trans. R. Soc.* A **240** 599
[2] Néel L 1949 *Ann. Géophys.* **5** 99
[3] Hernando A 1999 *J. Phys.: Condens. Matter* **11** 9455
[4] Michele O, Hesse J and Bremers H 2006 *J. Phys.: Condens. Matter* **18** 4921
[5] Hesse J, Graf T, Kopcewicz M, Afanas'ev A M and Chuev M A 1998 *Hyperfine Interact.* **113** 499
[6] Afanas'ev A M, Chuev M A and Hesse J 1997 *Phys. Rev.* B **56** 5489
[7] Afanas'ev A M, Chuev M A and Hesse J 1999 *JETP* **89** 533
[8] Brown W F Jr 1963 *Phys. Rev.* **130** 1677
[9] Chuev M A 2006 *JETP Lett.* **83** 572
[10] Tronc E, Ezzir A, Cherkaoui R, Chanéac C, Nougés M, Kachkachi H, Fiorani D, Testa A M, Grenèche J M and Joulivet J P 2000 *J. Magn. Magn. Mater.* **37** 39
[11] Jönsson P, Hansen M F and Nordblad P 2000 *Phys. Rev.* B **61** 1261
[12] Hesse J, Bremers H, Hupe O, Veith M, Fritscher E W and Valtchev K 2000 *J. Magn. Magn. Mater.* **212** 153
[13] Wernsdorfer W, Thirion C, Demoncy N, Pascard H and Mailly D 2002 *J. Magn. Magn. Mater.* **242–245** 132
[14] Rellinghaus B, Stappert S, Acet M and Wassermann E F 2003 *J. Magn. Magn. Mater.* **266** 142
[15] Cador O, Grasset F, Haneda H and Etournea J 2004 *J. Magn. Magn. Mater.* **268** 232
[16] Michele O 2004 *PhD Thesis* Technische Universität Braunschweig (http:opus.tu-bs.de/opus/volltexte/2005/46)
[17] Schrefl T 1999 *J. Magn. Magn. Mater.* **207** 45
[18] Sun Z Z and Wang X R 2005 *Phys. Rev.* B **71** 174430
[19] Henkel O 1964 *Phys. Status Solidi* **7** 919
[20] Thamm S and Hesse J 1996 *J. Magn. Magn. Mater.* **154** 254
[21] Michele O, Hesse J, Bremers H, Wojczykowski K, Jutzi P, Sudfeld D, Ennen I, Hütten A and Reiss G 2004 *Phys. Status Solidi* C1 **12** 3596
[22] Aharoni A 1969 *Phys. Rev.* **177** 793
[23] Pfeiffer L 1971 *J. Appl. Phys.* **42** 1725
[24] Michele O, Hesse J, Bremers H, Polychroniadis E K, Efthimiadis K G and Ahlers H 2004 *J. Phys.: Condens. Matter* **16** 427
[25] Chuev M A 2007 *JETP Lett.* **85** 611